

## Synthesis and Conformation–Activity Relationships of the Peptide Isoesters of FK228 and Largazole

Albert A. Bowers,<sup>†</sup> Thomas J. Greshock,<sup>†</sup> Nathan West,<sup>§,||</sup> Guillermina Estiu,<sup>∇</sup> Stuart L. Schreiber,<sup>||,⊥</sup> Olaf Wiest,<sup>\*,∇</sup> Robert M. Williams,<sup>\*,†,‡</sup> and James E. Bradner<sup>\*,§,||</sup>

Department of Chemistry, Colorado State University, Fort Collins, Colorado 80523, University of Colorado Cancer Center, Aurora, Colorado 80045, Division of Hematologic Neoplasia, Dana-Farber Cancer Institute, Boston, Massachusetts 02115, Chemical Biology Program, Broad Institute of Harvard and MIT, Cambridge, Massachusetts 02142, Howard Hughes Medical Institute, Chemistry and Chemical Biology, Harvard University, Cambridge, Massachusetts 02138, and Walther Cancer Research Center and Department of Chemistry and Biochemistry, University of Notre Dame, Notre Dame, Indiana 46556

Received October 2, 2008; E-mail: james\_bradner@dfci.harvard.edu

**Abstract:** The peptide isoesters (**10** and **11**) of the naturally occurring and potent histone deacetylase (HDAC) inhibitors FK228 and largazole have been synthesized and evaluated side-by-side with FK228, largazole, and SAHA for inhibition of the class I HDACs **1**, **2**, **3**, and **6**.

Histone deacetylase (HDAC) inhibitors are under intense investigation as targeted therapies for the treatment of cancer.<sup>1</sup> The zinc-dependent, class I hydrolases (HDAC1, 2, 3, 8) are implicated in numerous events associated with malignant transformation, notably epigenetic maintenance of the malignant phenotype. Numerous small-molecule HDAC inhibitors have been identified in nature or developed with medicinal chemistry. Several naturally occurring and synthetic HDAC inhibitors are shown in Figure 1 and include SAHA (**1**),<sup>2</sup> trichostatin A (**2**),<sup>2</sup> apicidin (**3**),<sup>4</sup> trapoxin B (**4**),<sup>3,4</sup> azumamide A (**5**),<sup>5–7</sup> FK228 (**6**),<sup>8–10</sup> FR901375 (**7**),<sup>8–10</sup> spiruchostatins (**8**),<sup>11</sup> and largazole (**9**).<sup>12–14</sup> A common pharmacophore model has been used to

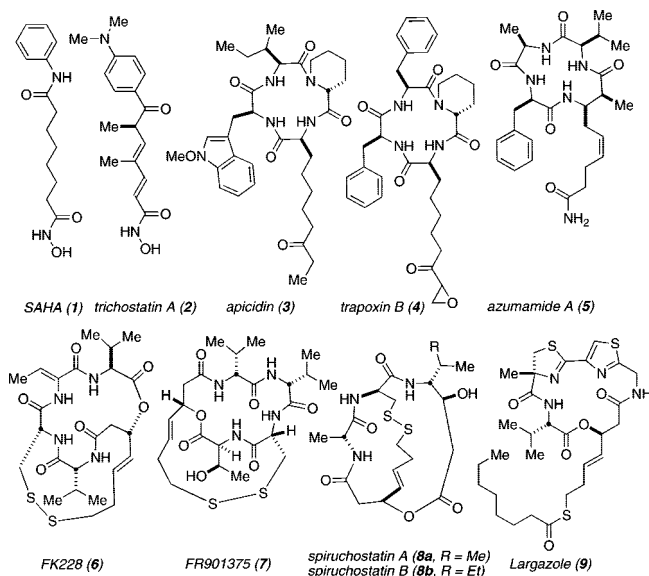


**Figure 1.** Several known potent HDAC inhibitors.

describe this set of seemingly diverse chemical probes: (1) a metal-binding domain, which interacts with the active-site Zn<sup>2+</sup>, (2) a predominantly hydrophobic linking group, which occupies the channel of the enzyme and mimics the histone protein *N*-acetyl-lysine side chain, and (3) a surface recognition domain.<sup>15</sup> The opportunity to study structure–activity relationships among HDAC inhibitors with more granularity has recently caught our attention. We specifically have become interested in the analogous depsipeptide natural products, FK228

- (13) Ying, Y.; Taori, K.; Kim, H.; Hong, J.; Luesch, H. J. *Am. Chem. Soc.* **2008**, *130*, 8455–9.  
 (14) Bowers, A.; West, N.; Taunton, J.; Schreiber, S. L.; Bradner, J. E.; Williams, R. M. *J. Am. Chem. Soc.* **2008**, *130*, 11219–22.  
 (15) Sternson, S. M.; Wong, J. C.; Grozinger, C. M.; Schreiber, S. L. *Org. Lett.* **2001**, *3*, 4239–42.

<sup>†</sup> Colorado State University.

<sup>‡</sup> University of Colorado Cancer Center.

<sup>§</sup> Dana-Farber Cancer Institute.

<sup>||</sup> Broad Institute of Harvard and MIT.

<sup>⊥</sup> Harvard University.

<sup>∇</sup> University of Notre Dame.

- (1) Minucci, S.; Pelicci, P. G. *Nat. Rev. Cancer* **2006**, *6*, 38–51.  
 (2) Yoshida, M.; Kijima, M.; Akita, M.; Beppu, T. *J. Biol. Chem.* **1990**, *265*, 17174–9.  
 (3) Kijima, M.; Yoshida, M.; Sugita, K.; Horinouchi, S.; Beppu, T. *J. Biol. Chem.* **1993**, *268*, 22429–35.  
 (4) Taunton, J.; Hassig, C. A.; Schreiber, S. L. *Science* **1996**, *272*, 408–11.  
 (5) Nakao, Y.; Yoshida, S.; Matsunaga, S.; Shindoh, N.; Terada, Y.; Nagai, K.; Yamashita, J. K.; Ganesan, A.; van Soest, R. W.; Fusetani, N. *Angew. Chem., Int. Ed.* **2006**, *45*, 7553–7.  
 (6) Izzo, I.; Maulucci, N.; Bifulco, G.; De Riccardis, F. *Angew. Chem., Int. Ed.* **2006**, *45*, 7557–60.  
 (7) Wen, S.; Carey, K. L.; Nakao, Y.; Fusetani, N.; Packham, G.; Ganesan, A. *Org. Lett.* **2007**, *9*, 1105–8.  
 (8) Ueda, H.; Nakajima, H.; Hori, Y.; Fujita, T.; Nishimura, M.; Goto, T.; Okuhara, M. *J. Antibiot. (Tokyo)* **1994**, *47*, 301–10.  
 (9) Shigematsu, N.; Ueda, H.; Takase, S.; Tanaka, H.; Yamamoto, K.; Tada, T. *J. Antibiot. (Tokyo)* **1994**, *47*, 311–4.  
 (10) Ueda, H.; Manda, T.; Matsumoto, S.; Mukumoto, S.; Nishigaki, F.; Kawamura, I.; Shimomura, K. *J. Antibiot. (Tokyo)* **1994**, *47*, 315–23.  
 (11) Yurek-George, A.; Habens, F.; Brimmell, M.; Packham, G.; Ganesan, A. *J. Am. Chem. Soc.* **2004**, *126*, 1030–1.  
 (12) Taori, K.; Paul, V. J.; Luesch, H. J. *Am. Chem. Soc.* **2008**, *130*, 1806–7.

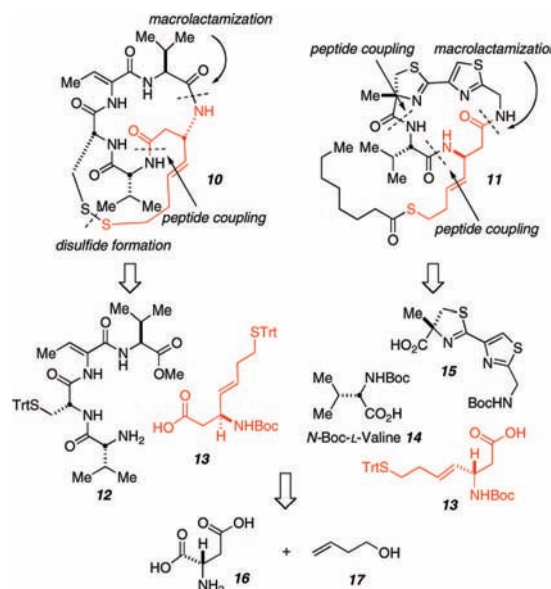
(6) and largazole (9). The unique, remarkable HDAC inhibition exhibited by these ligands suggests that the complex, macrocyclic capping region likely confers high-potency surface interactions. We sought to explore this hypothesis in comparing the biochemical activity and predicted conformational space of these two natural products with their corresponding peptide isosteres.

FK228 (6) was originally isolated from the fermentation broth of *Chromobacterium violaceum* (No. 968) by Fujisawa Pharmaceutical Co., Ltd. in 1991 along with the closely related depsipeptide, FR901375 (7). The unique structural features of FK228 include a 16-membered cyclic depsipeptide bridged by a 15-membered macrocyclic disulfide ring. The D-cysteine residue of the peptide portion enables FK228 to act as a pro-drug, in which the disulfide bond is reduced in vivo by glutathione reductase to reveal the butenyl thiol that is known to interact with zinc in the binding pocket of zinc-dependent class I/II histone deacetylases.<sup>16</sup> The potent activity of FK228 ( $IC_{50} = 0.2$  nM for FK228 against HDAC1)<sup>14</sup> against a range of murine and human solid tumor cells, as well as its ability to target epigenetic silencing mechanisms crucial to carcinogenesis, has culminated in its advancement into clinical trials as a potent anticancer therapy. Despite evident activity in cutaneous T-cell lymphoma, serious cardiac adverse events have been associated with FK228, which may limit expansive clinical development as a cancer therapeutic. Recently, a phase II study of FK228 in gastrointestinal neuroendocrine tumors was terminated due to sudden cardiac death.<sup>17a</sup> To gain additional insight into the biochemistry, activity, and toxicity of FK228, the generation of more synthetic material was required. Thus, we have recently completed a total synthesis of FK228,<sup>17b</sup> which we anticipate will be amenable to scaling and derivative synthesis in the near future.

Largazole (9) was recently isolated from the marine cyanobacterium, *Symploca* sp. by Luesch and co-workers.<sup>12</sup> Structural features of largazole closely resemble FK228, FR901375, and spiruchostatin. Each possesses a 16-membered depsipeptide macrocycle and an appending (*S*)-3-hydroxy-7-mercaptohept-4-enoic acid residue. Biological studies of largazole established a potent antiproliferative effect in panels of human and murine cancer cell lines in vitro.<sup>12,14</sup> These attributes inspired several research groups, including ours, to complete the total synthesis of largazole and to assess biochemical potency of the natural product and key derivatives against human deacetylases.<sup>13,14,18</sup> These studies collectively establish largazole as a thioester pro-drug HDAC inhibitor, which is likely activated by metabolic hydrolysis of the octanoyl residue. We and others have prepared the thiol derivative (largazole thiol) and reported potent biochemical inhibition of class I HDACs ( $IC_{50} = 0.1$  nM against HDAC1).<sup>14</sup>

The hydroxamic acid metal chelator is widely considered the highest activity ligand for zinc, yet we and others have observed remarkable, unprecedented biochemical potency of thiol derivatives of natural product, pro-drug HDAC inhibitors.<sup>14</sup> We postulate that this potency derives either (or mutually) from favorable nonbonded interactions between the surface recogni-

**Scheme 1.** Retrosynthesis of FK228 and Largazole Peptide Isosteres

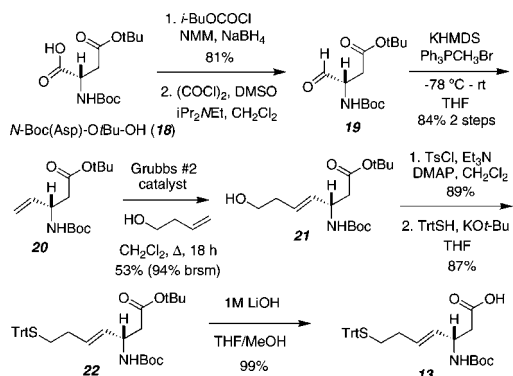


tion domain and receptor, as we and others have observed with other HDAC inhibitors,<sup>19</sup> or from the accessible conformational space imposed by macrocyclic constraints. Building on the newly afforded synthetic accessibility of FK228 and largazole, we sought to explore conformation–activity relationships in the active depsipeptide derivatives of FK228 and largazole, and their respective amide isosteres. The amide isosteres were immediately envisioned to offer more hydrolytic stability, as well as conformational rigidity to these molecular scaffolds as compared with their depsipeptide progenitors.

As a first step in this process, herein we wish to report the syntheses of the amide isosteres of FK228 (10) and largazole (11). Given the results of prior art on FK228 and largazole, the isostere syntheses presented two key challenges: (1) the preparation of the enantiomerically pure  $\beta$ -amino acid analogue of the (*S*)-3-hydroxy-7-mercaptohept-4-enoic acid common to both substrates and (2) ring-closure of these new macrocyclic peptides, which would likely differ from their depsipeptide progenitors in conformational rigidity and therefore transition state energy (Scheme 1). The stereochemistry of the novel  $\beta$ -amino acid we envisioned incorporating would derive from a selectively protected aspartic acid derivative. Elaboration of this building block via olefination/homologation would likely provide rapid and scalable access to the desired fragment. From the  $\beta$ -amino acid, completion of the cyclization precursors were patterned after our established syntheses of the two parent compounds. In the case of the FK228 isostere, coupling of carboxylic acid 13 to peptide 12<sup>20</sup> would provide a cyclization precursor ready for ligation at the least-hindered amide ring juncture.<sup>21,22</sup> Our laboratories have recently developed a modified synthesis of peptide 12, which has proven successful for its preparation on up to a 20-g scale.<sup>17b</sup> The disulfide bridge

(16) Furumai, R.; Matsuyama, A.; Kobashi, N.; Lee, K. H.; Nishiyama, M.; Nakajima, H.; Tanaka, A.; Komatsu, Y.; Nishino, N.; Yoshida, M.; Horinouchi, S. *Cancer Res.* **2002**, *62*, 4916–21.  
 (17) (a) Shah, M. H.; Brinkley, P.; Chan, K.; Xiao, J.; Arbogast, D.; Collamore, M.; Farra, Y.; Young, D.; Grever, M. *Clin. Cancer Res.* **2006**, *12*, 3997–4003. (b) Greshock, T. J.; Johns, D. M.; Noguchi, Y.; Williams, R. M. *Org. Lett.* **2008**, *10*, 613–6.  
 (18) Ghosh, A. K.; Kulkarni, S. *Org. Lett.* **2008**, *10*, 3907–9.

(19) Estiu, G.; Greenberg, E.; Harrison, C. B.; Kwiatkowski, N. P.; Mazitschek, R.; Bradner, J. E.; Wiest, O. *J. Med. Chem.* **2008**, *51*, 2898–906.  
 (20) Li, K. W.; Wu, J.; Xing, W.; Simon, J. A. *J. Am. Chem. Soc.* **1996**, *118*, 7237–7238.  
 (21) Davies, J. S. *J. Pept. Sci.* **2003**, *9*, 471–501.  
 (22) Humphrey, J. M.; Chamberlin, A. R. *Chem. Rev.* **1997**, *97*, 2243–2266.

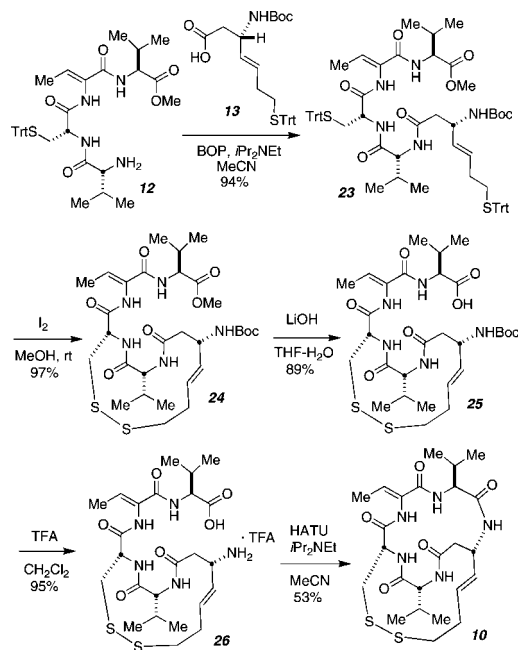
Scheme 2. Synthesis of  $\beta$ -Amino Acid **13**

could be installed last by an oxidative deprotection of the bis(thiotrityl) peptide and concomitant cyclization to form the 15-membered ring. Similarly, the largazole substrate could be assembled from *N*-Boc-*L*-valine and thiazoline-thiazole acid **15**, allowing ring closure between the sterically unencumbered acid and its primary amino-terminus.

Our synthesis of the requisite  $\beta$ -amino acid side chain **13** began with a reduction of the *iso*-butyl mixed anhydride derivative of commercially available Boc(Asp)-*O**t*Bu-OH (**18**) with NaBH<sub>4</sub> to produce the corresponding primary alcohol (Scheme 2). This alcohol was then subjected to Swern oxidation conditions giving rise to aldehyde **19**. It should be noted that aldehyde **19** proved to be an extremely difficult compound to handle since it was prone to racemization immediately following workup. Fortunately, a workup procedure for the corresponding *N*-Cbz derivative of aldehyde **19** published by Zappia and co-workers<sup>23</sup> involving aqueous KHSO<sub>4</sub> proved successful in preventing racemization of **19**. Following workup, aldehyde **19** was immediately subjected to a Wittig reaction with methyl-enetriphenylphosphorane to furnish alkene **20** as a single enantiomer in 84% yield over two steps.

The butenyl side chain was next introduced via a cross metathesis reaction with 3-buten-1-ol in the presence of Grubbs second generation catalyst<sup>24</sup> to provide alcohol **21**, exclusively as the *trans*-olefin in 53% yield, along with 41% recovered starting material which can be easily separated and recycled in another cross metathesis reaction. Attempts to prepare the *trans*-butenyl alcohol **21** directly from aldehyde **19** via a Wittig reaction of the ylide derived from 3-iodopropanol proved unsuccessful, resulting in decomposition of starting material. Although recently reported syntheses of largazole have utilized a late-stage metathesis on an olefin-functionalized macrocycle,<sup>13,18,25</sup> the yields have been substantially encumbered by the intrinsic steric hindrance. During our research toward this synthesis,<sup>14,17b</sup> that were initiated well before the reported isolation of largazole, we chose to complete the metathesis early, to avoid late-stage loss of material and to provide this single building block in quantities compatible with analogue screening of variations in the macrocycle itself. Alcohol **21** was successfully transformed to the desired  $\beta$ -amino acid **13** in a short three-step sequence, via *t*-butyl ester **22**.

With the key precursors in hand, we next directed our attention toward the assemblage of  $\beta$ -amino acid **13** with

Scheme 3. Construction of the FK228 Peptide Isostere **10** via a Macrolactamization Reaction

tetrapeptide **12** and the ensuing completion of the desired FK228 analogue **10**. Accordingly, peptide **12** was effectively coupled with acid **13** in the presence of BOP reagent and Hünigs base to afford ester **23** (Scheme 3). We had originally intended to perform the macrolactamization reaction prior to disulfide ring formation, just as Simon and co-workers<sup>20</sup> had done to form the depsipeptide in their FK228 total synthesis. Unfortunately, all conditions attempted to effect a macrolactamization reaction on the free amino acid salt corresponding to methyl ester **23**, proved unsuccessful. A variety of peptide coupling reagents,<sup>21,22</sup> solvents, bases, and temperatures were employed, but only traces of the desired macrocycle were ever recovered from the reaction.

As an alternative strategy, we then focused our attention on closure of the disulfide ring *prior* to the macrolactamization reaction. We felt that the additional rigidity provided by the 15-membered disulfide ring could tilt the uphill battle with entropy in our favor and allow cyclization to the 16-membered peptide ring. Thus, peptide **23** was treated with iodine in MeOH to effect an oxidative deprotection of the bis(thiotrityl) groups and concomitant cyclization to the 15-membered disulfide ring giving rise to compound **24** in excellent yield. The ester group of **24** was then saponified with LiOH producing acid **25**.

The Boc group was subsequently removed in the presence of TFA, and following concentration of the reaction mixture, amino acid TFA salt **26** was obtained in excellent yield. We were gratified to discover that amino acid **26** was a suitable substrate for the desired macrolactamization reaction. Treatment of **26** with HATU and Hünigs base in CH<sub>3</sub>CN successfully produced the FK228 peptide isostere **10** in 53% yield. The reaction appeared to run even more smoothly when BOP was used as the coupling reagent; however, removal of the HMPA byproduct proved difficult by either aqueous HCl wash or silica gel chromatography.

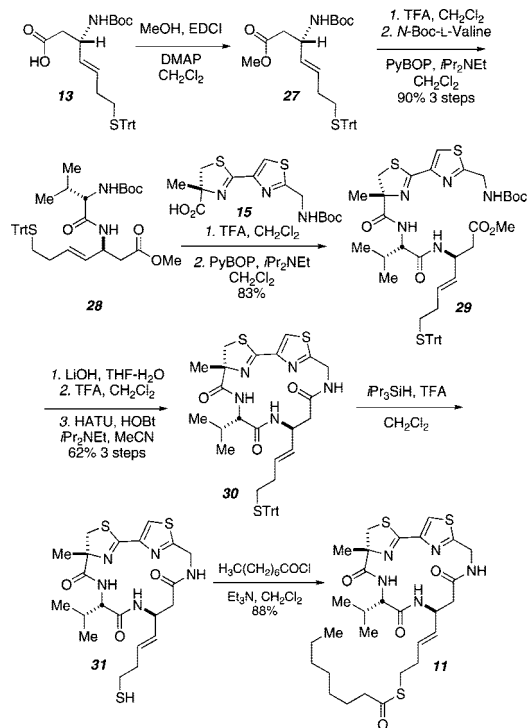
Our route to the largazole amide isostere (**11**) followed closely that of our recently reported synthesis of largazole itself (Scheme 4). Thus,  $\beta$ -amino acid **13** was converted to its methyl ester, deprotected, and coupled to *N*-Boc-*L*-valine to provide peptide **28**. Further deprotection of this subunit and coupling to

(23) Delle Monache, G.; Misiti, D.; Salvatore, P.; Zappia, G. *Chirality* **2000**, *12*, 143–8.

(24) Scholl, M.; Ding, S.; Lee, C. W.; Grubbs, R. H. *Org. Lett.* **1999**, *1*, 953–6.

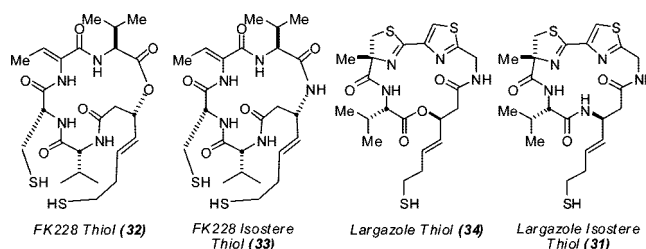
(25) Nasveschuk, C. G.; Ungermannova, D.; Liu, X.; Phillips, A. J. *Org. Lett.* **2008**, *10*, 3595–8.



**Scheme 4.** Construction of the Largazole Peptide Isostere **11** via a Macrolactamization Reaction

thiazoline-thiazole amino acid **15**<sup>14</sup> gave acyclic precursor **29** in 83% yield. Initial attempts at macrocyclization according to the same procedures that provided largazole gave a 30% yield of macrocycle **30**, together with large amounts of a dimeric product. A revised procedure was developed in which the TFA salt of the acyclic precursor was first neutralized by stirring in acetonitrile/Hünig's base and then added via syringe pump over 10 h to a dilute solution of HOBT/HATU in acetonitrile. This procedure resulted in a 62% yield of the desired macrocycle, which was then deprotected to yield the largazole isostere thiol (**31**). Acylation of the thiol completed the synthesis of the largazole peptide isostere (**11**).

For biochemical studies profiling the comparative potency of these small-molecule inhibitors of human HDACs, we have miniaturized and further optimized a homogeneous trypsin-coupled assay<sup>14,19,26</sup> (see Supporting Information, Figure S1). This fluorogenic assay provides kinetic measurements of deacetylase function and has previously proven compatible with high-throughput screening, directing medicinal chemistry, and correlative molecular dynamics studies.<sup>19</sup> Recognizing that reduction of disulfide bond formation would be necessary to accurately measure enzyme inhibition by FK228 and its amide isostere, we sought to adapt the assay for performance under reducing conditions. We were surprised to observe confounding deacetylase inhibition by those reducing agents used most commonly in experimental biology (dithiothreitol and  $\beta$ -mercaptoethanol; Supporting Information, Figure S2A, B). Furthermore, substantial enzyme inhibition was observed at concentrations of these agents required to activate FK228, presumably by reduction of the disulfide bond as described (Supporting Information, Figure S2C).<sup>16</sup> In contrast, tris(2-carboxyethyl)-phosphine hydrochloride (TCEP) demonstrated comparably weak enzyme inhibition

**Figure 2.** Biochemically active forms of the HDAC inhibitors.**Table 1.** HDAC Inhibitory Activity ( $IC_{50}$ ; nM) of Thiol Depsipeptides and Peptide Isosteres

compound	HDAC1	HDAC2	HDAC3	HDAC6
FK228 ( <b>6</b> )	0.2	1	3	200
FK228 isostere ( <b>10</b> )	10	80	70	>3000
largazole thiol ( <b>34</b> )	0.1	0.8	1	40
largazole ( <b>9</b> ) <sup>a</sup>	40	42	96	>1000
largazole isostere thiol ( <b>31</b> )	0.9	4	4	1500
largazole isostere ( <b>11</b> )	>3000	>3000	>3000	>3000
SAHA ( <b>1</b> )	10	40	30	30

<sup>a</sup> The largazole sample used in this study was synthesized in these laboratories and purified to homogeneity. Biochemical data included herein have been previously reported by our laboratories and are provided for direct comparison.<sup>14</sup>

at concentrations markedly higher than that required to activate FK228 (Supporting Information, Figure S2B, C). We selected ideal reducing conditions with TCEP at 200  $\mu$ M.

In a parallel assay format, we then profiled the potency of the depsipeptide natural product HDAC inhibitors versus their respective peptide isosteres, all as 'active' thiols (Figure 2). FK228 and the FK228 amide isostere are activated to the corresponding thiols (**32** and **33**, respectively) under reducing conditions. Largazole thiol and the corresponding isostere were prepared by organic synthesis as above and as we have previously described.<sup>14</sup>

We selected for study HDAC1 (1.67 ng/ $\mu$ L), HDAC2 (0.067 ng/ $\mu$ L), HDAC3 (0.033 ng/ $\mu$ L), and HDAC6 (0.67 ng/ $\mu$ L). HDAC3 was studied in reflection of its biologically active complex with a peptide fragment of the nuclear corepressor (NCoR2; BPS Biosciences). We were pleased to observe comparable deacetylase inhibitory activity for control compounds, such as SAHA (Table 1), as recently reported in the scientific literature.<sup>27</sup> In addition, the high potency of synthetic FK228 (HDAC1  $IC_{50}$  0.2 nM) in this assay recapitulates prior data from our groups highlighting assay robustness and reproducibility.<sup>14</sup>

A striking observation emerged from these experiments. Comparable potencies are observed between FK228 and largazole thiol, as expected. Again, we observed remarkable, subnanomolar potency against HDAC1 and affirm the pro-drug hypothesis of both natural products. However, disparate potencies are observed between their respective peptide isosteres. As demonstrated in Figure 3, the amide isostere of FK228 is 50-fold less potent an inhibitor of HDAC1 than is the natural product.

The peptide isostere of largazole thiol (**31**) is, indeed, reduced in potency for HDAC1 compared to the natural product, but only by 9-fold (Figure 3). The trend of increased potency for

(26) Vegas, A. J.; Bradner, J. E.; Tang, W.; McPherson, O. M.; Greenberg, E. F.; Koehler, A. N.; Schreiber, S. L. *Angew. Chem., Int. Ed.* **2007**, *46*, 7960–4.

(27) Pescatore, G.; Kinzel, O.; Attenu, B.; Cecchetti, O.; Fiore, F.; Fonsi, M.; Rowley, M.; Schultz-Fademrecht, C.; Serafini, S.; Steinkuhler, C.; Jones, P. *Bioorg. Med. Chem. Lett.* **2008**.

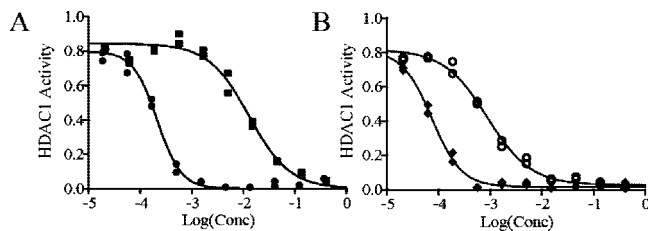


**Figure 3.** Biochemical inhibition of HDAC1. (A) Replicate dose-ranging studies of FK228 (closed circles) and the peptide isostere (squares). (B) Replicate dose-ranging studies of largazole thiol (diamonds) and largazole isostere thiol (open circles).

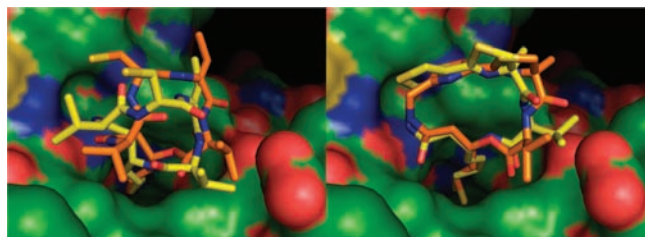


**Figure 4.** Coordination mode of FK228 (left) and largazole thiol (right) to the HDAC1 active site. Depsideptides are shown in orange, and amide isosteres are shown in yellow.

the largazole peptide isostere thiol versus the FK228 peptide isostere was preserved across all human class I HDACs tested (Table 1).

The finding that the FK228 amide isostere (**10**) is 50-fold less active against HDAC1 than FK228 could be explained by two different hypotheses. The replacement of the ester by an amide could change the hydrogen-bonding pattern and thus the binding constant in analogy to the development of resistance to the macrocyclic glycopeptide antibiotic, vancomycin. Alternatively, replacement of the ester by an amide could alter the accessible conformational space. The stronger effect of substitution observed for FK228 than largazole renders the first hypothesis less likely. Nonetheless, we decided to deploy computational methods to study the effects of isostere replacement and model the disparate observed target potencies.

We employed a strategy where the conformational space of the free thiols of FK228 (**32**), FK228 amide isostere (**33**), largazole (**34**), and largazole isostere (**31**) was determined by a Monte Carlo conformational search. Subsequent structural clustering was performed according to the heavy atoms root-mean-squared (rms) value. Average structures for each cluster were docked to the previously studied homology model of HDAC1<sup>28–30</sup> using Glide XP<sup>31</sup> to probe the binding site with each discrete small-molecule conformer.

The preferred coordination modes of the four analyzed structures are presented in Figure 4. The thiol extends toward the zinc ion at the bottom of the entrance channel with a Zn–S distance of  $\sim 2.5$  Å while the macrocycle sits on the mouth of the pocket. The hydrocarbon chain fills the hydrophobic channel, with the unsaturated bond lined by Phe150 and Phe205 in a

**Table 2.** Energy Differences of the Average Structures of the Clusters Grouped by Heavy Atom rms Values, Relative to the Most Stable Cluster of Each Compound<sup>a</sup>

cluster	FK228 ( <b>32</b> )	FK228 isostere ( <b>33</b> )	largazole ( <b>34</b> )	largazole isostere ( <b>31</b> )
1	0 (0)	0 (0)	0 (0)	0 (0)
2	28 (3.8)	13 (3.71)	30 (2.27)	39 (3.33)
3	35 (3.5)	31 (3.17)	35 (2.29)	<b>48 (1.41)</b>
4	35 (4.2)	30 (2.55)	49 (2.89)	22 (3.27)
5	37 (3.8)	41 (2.39)	35 (3.26)	43 (2.65)
6	<b>5 (1.8)</b>	45 (4.7)	49 (2.77)	28 (2.78)
7	39 (2.7)	<b>40 (3.11)</b>	27 (3.15)	33 (2.06)
8	36 (2.6)		32 (3.58)	
9	32 (3)		38 (3.18)	
10	21 (2.5)		37 (4.09)	
11	30 (2.5)			
12	32 (3.5)			

<sup>a</sup> Energetic data (kJ/mol) are presented with rms data in parentheses. Preferred conformations for coordination to HDAC1 are presented in boldface type.

parallel arrangement. It is important to note that the orientation of the macrocycle is similar in the ester and the amide isostere, maximizing lipophilic interactions with residues of the cap. Changes in the hydrogen-bonding pattern between the natural products and their amide isosteres do not appear to play a role because this moiety is positioned in a hydrophobic region of the pocket. The similar coordination mode of the ester and the amide isostere thus does not help to understand their different deacetylase activity.

The experimental data can be understood, however, by comparing the average structure of each conformational cluster with the structure associated with the lowest energy pose, i.e., the preferred coordination to the HDAC1 active site. Table 2 summarizes the results of the conformational search for the four compounds under study. We present the energy of the clusters (in kJ/mol), as well as the heavy atom rms relative to the most stable conformation. This analysis reveals a small predicted energy difference between the free (cluster 1) and bound (cluster 6) conformation of FK228 thiol. The small energy difference (5 kJ/mol) between the bound conformations could be easily compensated by the binding energy to the protein. This may be further understood in the context of the geometries, shown in Figure 4 and the low rms of 1.77 Å between the bound and the low-energy conformations. In contrast, the amide isostere is much more rigid, as revealed by the relatively few ( $n = 7$ ) geometries afforded by the 50 kJ/mol window considered here. Furthermore, the preferred geometry for binding (cluster 7) is considerably higher in energy (40 kJ/mol) than the energetically favored pose (cluster 1), and the two conformations comprise radically different geometries. This is appreciated qualitatively in Figure 5 and quantitatively (rms = 3.11 Å) in Table 2.

There are, in fact, no conformations that are energetically accessible and resemble the bound conformations. Binding of the FK228 isostere thiol (**33**) will therefore involve a significant distortion of the protein surface and loss of binding interactions, leading to the experimentally observed loss of activity.

In the case of largazole thiol (**34**), the lowest energy conformation is, in fact, the preferred binding conformation (cluster 1). Otherwise stated, the structure of the best pose perfectly overlays the average structure of the cluster with the lowest energy (Figure 4). In the case of the amide isostere, on the other hand, the ideal structure for docking (active conformation) overlaps with cluster 3, which is 48 kJ/mol higher in energy than the most stable conformation of the unbound species (cluster 1). Binding is hence also favored for the ester over the

(28) Wang, D. F.; Helquist, P.; Wiech, N. L.; Wiest, O. *J. Med. Chem.* **2005**, *48*, 6936–47.

(29) Wang, D. F.; Wiest, O.; Helquist, P.; Lan-Hargest, H. Y.; Wiech, N. L. *J. Med. Chem.* **2004**, *47*, 3409–17.

(30) Weerasinghe, S. V.; Estiu, G.; Wiest, O.; Pflum, M. K. *J. Med. Chem.* **2008**, *51*, 5542–51.

(31) Friesner, R. A.; Murphy, R. B.; Repasky, M. P.; Frye, L. L.; Greenwood, J. R.; Halgren, T. A.; Sanschagrin, P. C.; Mainz, D. T. *J. Med. Chem.* **2006**, *49*, 6177–96.

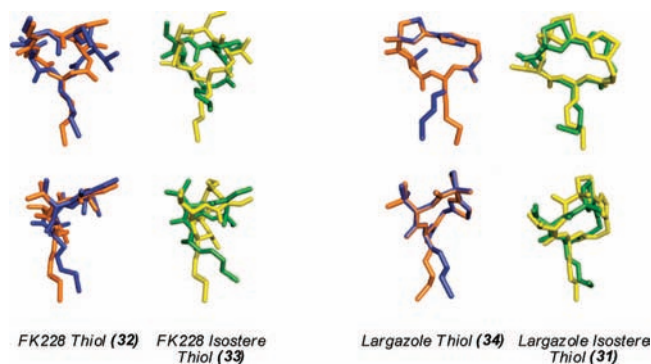


**Figure 5.** Top and side view of superimposed lowest energy binding conformations (orange for FK228 and largazole, yellow for peptide isosteres) and the average structure for the cluster of lowest energy (blue for desipeptides and green for peptide isosteres).

amide isostere. However, it is notable that the geometry between the most stable and most ideal binding conformation is relatively similar, as demonstrated by a low rms of 1.41 Å and comparison of the geometries in Figure 5. As a result, the conformational change of the protein required to accommodate the productive interaction with the macrocycle cap is relatively small, and much of the binding interaction will be maintained even if the low-energy conformation is bound. The deleterious effect of isostere substitution in the largazole thiol macrocycle, therefore, is predicted to be more modest than in FK228 thiol, which is in agreement with the experimental results.

In conclusion, we have established synthetic routes to the peptide isosteres of FK228 and largazole. Detailed profiling studies of class I/II deacetylases have confirmed the potent HDAC inhibition and a selective bias for class I enzymes. Using these chemical probes, we have demonstrated that subtle

differences in the chemical structure of the macrocyclic cap of natural product HDAC inhibitors may confer marked changes in accessible conformational space accounting for changes in inhibitor potency. This analysis shows how not only individual molecules but also the individual conformations can be correlated to experimentally observed activity so as to probe the binding site. This work importantly establishes a facile route to derivatives of each natural product which may now be further optimized toward unique patterns of isoform specificity and/or a potentially improved therapeutic window. Additionally, we establish a template strategy for integrated chemical, biological, and computational approaches to further modulating ligand potency, isoform selectivity, and druglike properties, which is the focus of our present studies.

**Acknowledgement.** We thank the Colorado State University Cancer Supercluster and the National Institutes of Health for financial support and the NIH National Cancer Institute for postdoctoral fellowship support for A.A.B. (Grant No. CA136283). Mass spectra were obtained on instruments supported by the NIH Shared Instrument Grant No. GM49631. O.W. and G.E. thank the Walther Cancer Research Center for financial support. We thank Ralph Mazitschek for the provision of acetylated substrates and helpful discussions. J.E.B. acknowledges support by grants from the National Cancer Institute (1K08CA128972) and the Burroughs-Wellcome Foundation (CAMS).

**Supporting Information Available:** Spectroscopic data and experimental details for the preparation of all new compounds, as well as procedures for the biochemical HDAC assay used in these experiments. This material is available free of charge via the Internet at <http://pubs.acs.org>.

JA80772W